# Electric and Magnetic Dual Meshes to Improve Moment Method Formulations

**M. Felipe Cátedra, Oscar Gutiérrez, Iván González, and Francisco Saez de Adana**

Computer Sciences Department, Universidad de Alcalá,
28806 Alcalá de Henares, Spain
felipe.catedra@uah.es

*Abstract* – A new Moment Method (MM) scheme to solve the Electric Field Integral Equation (EFIE) for some ill-conditioned problems is presented. The approach is an alternative to the Combined-Field Integral Equation (CFIE). The proposed formulation employs the Impedance Boundary Condition (IBC) to compute the scattering from conducting bodies uncoated or coated by dielectric materials. The scheme uses dual meshes to represent the currents: one mesh for the electric current and another mesh for the magnetic current. Each mesh is defined by a grid of quadrangles that can be conformed to arbitrarily curved surfaces. The quadrangle grids are interlocked; the corners of the quadrangles of one mesh are the centers of the quadrangles of the other mesh and vice versa. Several examples showing the potential of the approach to solve ill-conditioned problems are included.

## I.   INTRODUCTION

It is well known that many electromagnetic radiation or scattering problems can be too ill-conditioned to be solved using MM. This happens, particularly, when we analyze electrically large bodies using formulations based on either the EFIE or the Magnetic-Field Integral Equation (MFIE). In these cases, the MM equation systems are ill-conditioned at the resonance frequencies of the internal cavity defined by the volume of the body under analysis [1]. In these situations it is difficult to find reliable solutions, and thus these problems suffer from poor convergence and present spurious solutions.

To reduce the difficulty of these ill-conditioned problems, several formulations have been proposed to improve the condition number of the corresponding MM matrix that may help solve these problems. One of the most powerful formulations to avoid in these ill-conditioned problems is the CFIE, which is based on a linear combination of the EFIE and the MFIE, [1], [2]. Like the MFIE, the CFIE is only applicable to closed bodies. The practice has shown that the CFIE is able to treat most problems, however there are still cases where difficulties remain because the accuracy of CFIE results depend on a correct choice in the weights of the EFIE and MFIE linear combination, and on the sampling density (number of MM subdomains per wavelength) [3]. In these cases, convergence studies on the relative weights of the CFIE and on the sampling density are performed in order to obtain "stable" solutions. These difficulties can be due to the MFIE component of the CFIE which gives poor results for sharp wedges and tips, [4].

More recently formulations based on Dual-Surface Field Integral Equations (DSFIE), [5], [6] have been investigated because they appear to be free of spurious problems and offer better solutions for bodies with sharp wedges or tips. The DSFIE forces boundary conditions on the body surface and also in a dual surface located inside the body. The separation between the surfaces is usually less than half a wavelength, and on the dual surface the boundary conditions are multiplied by a constant with an imaginary part. The DSFIE reduces spurious resonances and can treat geometries with sharp parts like cone-spheres with narrow vertices where the CFIE does not yield reliable results. However, a suitable definition of the dual surface in the DSFIE application for a particular problem needs to be adjusted in order to obtain accurate results [6]. For electrically small objects, the approach in [7], [8], which uses an accurate computation of the MM matrix terms of the MFIE and monopolar basis functions, gives reliable computations for problems with sharp wedges and tips.

Here, a numerical scheme based on a combination of the EFIE and the IBC approach, [9-11] is presented as an alternative formulation to solve these difficult problems.

The scheme, outlined in [12], uses dual quadrangular meshes. One mesh is used to represent the discretized electric current and the other to represent the discretized magnetic current. The corners of the quadrangles of one mesh are in the centers of the quadrangles of the other mesh and vice versa. The scheme combines the operator which generates the electric field due to an electric current with the operator which generates an electric field due to a magnetic current. Both currents are expanded in terms of rooftop basis functions [13]. The testing functions are blade functions, [13], defined in the mesh used to represent the electric current. With this

choice of testing and basis functions we have found a simple and accurate way to descritize the electric field due to electric and magnetic currents. The meshes are defined over the iso-parametric lines of a NURBS´s (Non Uniform Rational Bi-Spline Surface) [14]. Using the discretization procedure shown in [15-17] we can work with curved quadrangles and we do not need any re-meshing in terms of flat patches.

One objective of our approach is to analyze real conducting bodies. It can be noticed that at microwave frequencies the surface impedance of a good conductor is a hundredth or a thousandth of the free space wave impedance and the solution for a good conductor at such frequencies is very similar to the case of a perfect electric conducting (PEC) body. Therefore, the proposed approach can give good results for PEC if we model PEC with a surface impedance of about a thousandth of the free space wave impedance. One of the advantages of the present approach is that it permits the analysis of open or closed surfaces or a combination of them. The proposed approach can be considered as a regularization method, [18-19], because it diminishes the Q factor of the internal cavities of closed bodies and in this way the formulation reduces the problems of spurious responses at resonances frequencies. In addition, the approach is able to treat accurately problems with sharp wedges and tips using a reduced number of samples per wavelength. It is also useful in analyzing the scattering from lossy dielectric or conducting bodies that can be totally or partially coated by thin materials using the IBC approach.

Dual meshes of quadrangles over curved surfaces are also considered in [20] to solve a CFIE in problems with dielectric bodies. In this reference, divergence-conforming basis functions are defined over one mesh and curl-conforming basis functions over the other mesh. Either current (electric or magnetic) is represented by both types of basis functions: divergence-conforming functions when the electric(magnetic) field of an electric(magnetic) current is computed, and curl-conforming basis functions when the magnetic(electric) field of an electric(magnetic) current is evaluated. Our approach is different from that of [20] because we solve the EFIE for metallic or body governed by the IBC and therefore, we can consider open and closed surfaces. Furthermore, we only use divergence-conforming functions in such a way that each mesh is reserved to only one kind of current, one mesh for the electric current and the other one for the magnetic current.

The paper is organized as follows; section 2 presents the theoretical formulation of the EFIE considered. The dual meshes and the numerical details of the method are shown in section 3. Some results that probe the capability of the approach to solve coated bodies, and ill-conditioned problems are presented in section 4, finally, the conclusion section.

## II. FORMULATION

We formulated the integral equation to be solved based on the equivalence principle, [21]. Figure 1 shows the application of the equivalence principe to obtain the fields in the region external to volume V. On the surface S that encloses volume V the equivalent currents are given by

$$\vec{J}_S(\vec{r}) = \hat{n}(\vec{r}) \times \vec{H}_T(\vec{r}), \tag{1.a}$$

$$\vec{M}_S(\vec{r}) = -\hat{n}(\vec{r}) \times \vec{E}_T(\vec{r}) \tag{1.b}$$

where $\vec{r} = r_x \hat{x} + r_y \hat{y} + r_z \hat{z}$ is the observation point on S and $(\vec{E}_T, \vec{H}_T)$ are the total fields that are in the region external to V and can be expressed as,

$$\vec{E}_T(\vec{r}) = \vec{E}^{imp}(\vec{r}) + \vec{E}^S(\vec{r}), \tag{2.a}$$

$$\vec{H}_T(\vec{r}) = \vec{H}^{imp}(\vec{r}) + \vec{H}^S(\vec{r}) \tag{2.b}$$

where $(\vec{E}^{imp}, \vec{H}^{imp})$ are the fields due to the impressed currents $(\vec{J}^{imp}, \vec{M}^{imp})$ located outside V and $(\vec{E}^S, \vec{H}^S)$ are the scattered fields due to the equivalent currents $(\vec{J}_S, \vec{M}_S)$
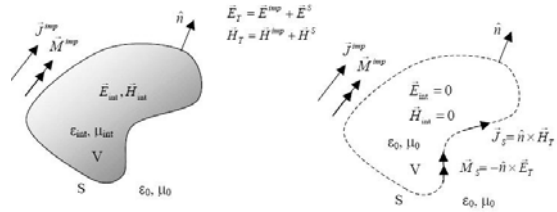


Fig. 1. The equivalence principle states that the field external to volume V in the problem shown in the left part of the figure can be computed considering the equivalent problem shown to the right.

Writing the scattered fields as a function of the electric and magnetic equivalent density currents for the external region, we get,

$$\vec{E}^S(\vec{r}) = -j\omega \frac{\mu}{4\pi} \iint_S \vec{J}_S(\vec{r}\,')G(\vec{r},\vec{r}\,')ds\,'$$

$$-j\frac{1}{4\pi\omega\varepsilon}\nabla\left(\iint_S \nabla'\vec{J}_S(\vec{r}\,')G(\vec{r},\vec{r}\,')ds\,'\right) \tag{3.a}$$

$$-\nabla\times\left(\frac{1}{4\pi}\iint_S \vec{M}_S(\vec{r}\,')G(\vec{r},\vec{r}\,')ds\,'\right),$$

$$\vec{H}^S(\vec{r}) = \nabla \times \left( \frac{1}{4\pi} \iint_S \vec{J}_S(\vec{r}\,')G(\vec{r},\vec{r}\,')ds' \right)$$

$$- j\omega \frac{\varepsilon}{4\pi} \iint_S \vec{M}_S(\vec{r}\,')G(\vec{r},\vec{r}\,')ds'$$

$$- j\frac{1}{4\pi\omega\mu} \nabla \left( \iint_S \nabla'\vec{M}_S(\vec{r}\,')G(\vec{r},\vec{r}\,')ds' \right).$$

(3.b)

These expressions can be written in a more compact form using the following linear operator notation,

$$\vec{E}^S(\vec{r}) = L_{EJ}[\vec{J}_S] + L_{EM}[\vec{M}_S],$$  (4.a)

$$\vec{H}^S(\vec{r}) = L_{HJ}[\vec{J}_S] + L_{HM}[\vec{M}_S].$$  (4.b)

We can combine equations (2) and (4) to obtain the EFIE and MFIE formulations,

$$\vec{E}_T(\vec{r}) = \vec{E}^{imp}(\vec{r}) + \vec{E}^S(\vec{r})$$
$$= \vec{E}^{imp}(\vec{r}) + L_{EJ}[\vec{J}_S] + L_{EM}[\vec{M}_S],$$  (5.a)

$$\vec{H}_T(\vec{r}) = \vec{H}^{imp}(\vec{r}) + \vec{H}^S(\vec{r})$$
$$= \vec{H}^{imp}(\vec{r}) + L_{HJ}[\vec{J}_S] + L_{HM}[\vec{M}_S].$$  (5.b)

For the case of a non-PEC body, like a real conducting body, a lossy dielectric body or a conducting body coated by a dielectric, the EFIE can be written as,

$$\vec{M}_S(\vec{r}) = -\hat{n}(\vec{r}) \times \vec{E}^{imp}(\vec{r}) - \hat{n}(\vec{r}) \times L_{EJ}[\vec{J}_S]$$
$$- \hat{n}(\vec{r}) \times L_{EM}[\vec{M}_S].$$  (6)

By reordering the EFIE we have

$$\vec{E}^{imp}(\vec{r}) = -\hat{n} \times \vec{M}_S(\vec{r}) - L_{EJ}[\vec{J}_S] - L_{EM}[\vec{M}_S].$$  (7)

Taking advantage of the duality between operators, we can write

$$L_{EM}[\vec{M}_S] = \frac{1}{\varepsilon} \nabla \times \left( \frac{\varepsilon}{4\pi} \iint_S -\vec{M}_S(\vec{r}\,')G(\vec{r},\vec{r}\,')ds' \right)$$
$$= L_{HJ}^{dual}[-\vec{M}_S]$$  (8)

where $L_{HJ}^{dual}$ is obtained from $L_{HJ}$ substituting the permeability μ by the permittivity ε.

Using the IBC relation between the electric and magnetic currents,

$$\vec{J}_S(\vec{r}) = \hat{n} \times \frac{\vec{M}_S(\vec{r})}{Z_{sup}},$$  (9.a)

$$\vec{M}_S(\vec{r}) = -(\hat{n} \times \vec{J}_S(\vec{r}))Z_{sup},$$  (9.b)

we obtain the following expression of the EFIE, where we only have the current $\vec{J}_S$ as the unknown function

$$\vec{E}^{imp}(\vec{r}) = -L_{EJ}[\vec{J}_S] - \frac{\hat{n} \times (\hat{n} \times \vec{J}_S(\vec{r}))Z_{sup}}{2}$$
$$+ L_{EM}^c[(\hat{n} \times \vec{J}_S(\vec{r}))Z_{sup}]$$  (10)

where $Z_{sup}$ stands for the surface impedance of the body and $L_{EM}^c$ is the resulting operator after extracting the singular value of $L_{EM}$.

## III. COMPUTATIONAL METHOD

The continuous operators in equation (10) can be discretized using the Moment Method. The scheme described in [15-17] has been followed to descritize the operator $L_{EJ}[\vec{J}_S]$. Using this scheme the body surface is modelled by means of NURBS´s [14]. Considering u- and v-isoparameter lines, [17], each NURBS can be split into a mesh of small curved quadrangles. The solid lines of Fig. 2 are an example of a rectangular mesh over a NURBS, which has been represented to be flat to simplify the drawing. The same figure shows a second mesh that is dual of the first one. The electric current is expanded in terms of rooftops defined over pairs of contiguous rectangles in the mesh defined by the solid lines. This expansion can be written as,

$$\vec{J}_S(\vec{r}) = \sum_{j=1}^{Nju} I_{Ju}(j)\vec{f}_{Ej}^u(\vec{r}) + \sum_{j=1}^{Njv} I_{Jv}(j)\vec{f}_{Ej}^v(\vec{r})$$  (11.a)

where $\vec{f}_{Ej}^u(\vec{r})$ and $\vec{f}_{Ej}^v(\vec{r})$ are rooftop functions for the u and v-components, respectively, of the electric current (see Fig. 3). In a similar way, the magnetic current can be expressed in terms of the rooftop functions $\vec{f}_{Mj}^u(\vec{r})$ and $\vec{f}_{Mj}^v(\vec{r})$, defined over the magnetic mesh (see Fig. 3). For the magnetic current we have,

$$\vec{M}_S(\vec{r}) = \sum_{j=1}^{Nmu} I_{Mu}(j)\vec{f}_{Mj}^u(\vec{r}) + \sum_{j=1}^{Nmv} I_{Mv}(j)\vec{f}_{Mj}^v(\vec{r}).$$  (11.b)

We can notice that for each u-rooftop/v-rooftop of the electric current a v-rooftop/u-rooftop of the magnetic current can be found such that the two rooftops have the same centre, they are perpendicular and they have a "dual" shape (the length of one is the width of the other and vice versa). Using this duality between couples of rooftops and the IBC of equations (9) the following relations between the weights of the current expansion of equation (11) can be found,

$$I_{Mu}(j) = \frac{\Delta_{Mu}^{j}}{\Delta_{Jv}^{j}} \| (\hat{u} \times \hat{v}) \| Z_{\sup} I_{Jv}(j), \qquad (12.a)$$

$$I_{Mv}(j) = -\frac{\Delta_{Mv}^{j}}{\Delta_{Ju}^{j}} Z_{\sup} \| (\hat{u} \times \hat{v}) \| I_{Ju}(j), \qquad (12.b)$$

where it is assumed that the parameter coordinates have been chosen so that $(\hat{u} \times \hat{v}) \bullet \hat{n} \geq 0$, $\Delta_{Mu}^{j}, \Delta_{Jv}^{j}, \Delta_{Mv}^{j}$ and $\Delta_{Ju}^{j}$ are the widths of rooftops $\vec{f}_{Mj}^{u}(\vec{r})$, $\vec{f}_{Ej}^{v}(\vec{r})$, $\vec{f}_{Mj}^{v}(\vec{r})$ and $\vec{f}_{Ej}^{u}(\vec{r})$, respectively, and $\| (\hat{u} \times \hat{v}) \|$ is the amplitude of the vector product $(\hat{u} \times \hat{v})$. It is noticed that eventually $\hat{u}$ and $\hat{v}$ can not be orthogonal in real 3D space. However, following the IBC in equation (9) $I_{Mu}(j)$ will never depend on $I_{Ju}(j)$ because both currents are parallel (neither $I_{Mv}(j)$ will depend on $I_{Jv}(j)$). Moreover, the following relations between the total numbers of rooftops are satisfied,

$$Nmv = Nju, \qquad (13.a)$$

$$Nmu = Njv. \qquad (13.b)$$

The descritized operators can be expressed as,

$$L_{EJ}^{D}\left[\vec{J}_{s}\right] = V_{EJ}(i)$$
$$= \sum_{j=1}^{Nju} Z_{ij}^{J} I_{Ju}(j) + \sum_{j=1}^{Njv} Z_{ij}^{J} I_{Jv}(j), \qquad (14.a)$$

$$L_{EM}^{D}\left[\vec{M}_{s}\right] = V_{EM}(i)$$
$$= \sum_{j=1}^{Nmu} Z_{ij}^{M} I_{Mu}(j) + \sum_{j=1}^{Nmv} Z_{ij}^{M} I_{Mv}(j), \qquad (14.b)$$

where the total number of rooftops used to represent the electric or the magnetic currents is given by

$$N = Nju + Njv \qquad (15)$$

$Z_{ij}^{J}$ and $Z_{ij}^{M}$ represent the coupling between subdomains i and j of the electric and magnetic meshes, respectively. The terms $V_{EJ}(i)$ and

$V_{EM}(i)$ stand for the impressed voltage due to the electric and magnetic current, respectively, computed in the electrical subdomain i, using as testing function a razor-blade function [15-17]. Other testing procedures can be used such as a Galerkin testing function. However, we have chosen a test by the razor-blade function because it is very simple and it needs fewer computations than other approaches, [13].
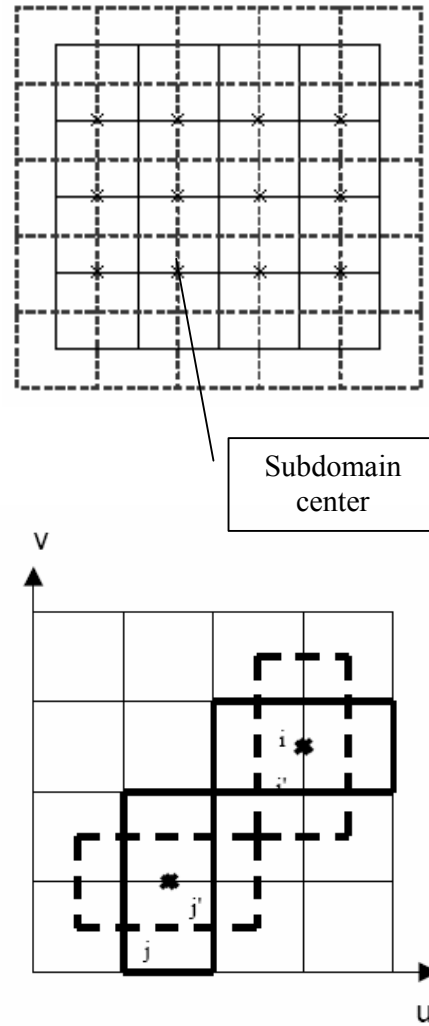


Fig. 2. A mesh of solid lines covers completely a NURBS. A second mesh is drawn using dashed lines. Both meshes are dual in the sense that the nodes of one mesh are the centres of the rectangles of the other mesh and vice versa.

The descritized operator $L_{EJ}^{D}$ of equation (14.a) can be obtained from the continuous operator $L_{EJ}$ of equation (7) following the numerical scheme shown in [13], [15-17]. The term $L_{EM}^{D}$ of equation (14.b) is obtained by descritizing the operator,

$$L_{EM}^T = -\frac{\hat{n} \times \bar{M}_S(\bar{r})}{2} - L_{EM}^c \left[ \bar{M}_S(\bar{r}) \right]. \qquad (16)$$

Considering the testing-function corresponding to an electric rooftop completely cuts its dual rooftop of magnetic current by a transversal line (see Fig. 4).

$$Z_{ij}^M = \begin{cases} sign(i)(\Delta i / 2) + Z_{ij}^c & for\ i = j \\ Z_{ij}^c & elsewhere \end{cases} \qquad (17)$$

where

$$sign(i) = \begin{cases} -1 & if\ subdomain\ i\ is\ a\ u-rooftop \\ 1 & if\ subdomain\ i\ is\ a\ v-rooftop \end{cases} \qquad (18)$$

and $\Delta i$ is the length of the razor-blade function of subdomain $i$ of the electrical mesh. The term $Z_{ij}^c$ accounts for the coupling between the magnetic rooftop $j$ and the electrical subdomain $i$ considering the operator $L_{EM}^c$ that gives the electric field of a magnetic current but excluding the singular value of the integral operator. The computation of the term $Z_{ij}^c$ does not have serious numerical difficulties and it can be calculated following a numerical approach similar to that indicated in [15-17] for the computation of $Z_{ij}^J$ .

Defining the total induced voltage $V(i)$ as,

$$V(i) = V_{EJ}(i) + V_{EM}(i) \qquad (19)$$

the following systems of linear equations can be obtained considering equations (12), (14) and (17)

$$V(i) = \sum_{j=1}^{Nju} (Z_{ij}^J - \frac{\Delta_{Mv}^j}{\Delta_{Ju}^j} Z_{sup} \|(\hat{u} \times \hat{v})\| Z_{ij}^M) I_{Ju}(j) +$$

$$+ \sum_{j=1}^{Njv} (Z_{ij}^J + \frac{\Delta_{Mu}^j}{\Delta_{Jv}^j} \|(\hat{u} \times \hat{v})\| Z_{sup} Z_{ij}^M) I_{Jv}(j);$$

$$for\ \ i = 1, 2, ... N \ .$$

$$(20)$$

Solving this system of linear equations the electric current is obtained. The magnetic current is obtained from the electric current using equation (12).

The approach is valid for problems defined by closed or open surfaces. When dealing with open surfaces the meshes near the aperture edges of the surfaces need to be defined in such a way so as to preserve the duality. Figures 5 and 6 show a way to define the meshes for a squared flat plate saving the duality between the electric and magnetic meshes. In both cases the rooftops of the two meshes cover completely the plate surface (the same domain), or in other words, the boundary of the meshes is the actual plate boundary. It can be noticed that the rooftops for

representing the electric and magnetic currents are spatially shifted but additionally they are defined near the edges of the plate in different ways: we have parallel and perpendicular rooftops for representing the electric current and these rooftops are defined over couple of patches of the same size, however we have not rooftops for representing the magnetic current parallel to the edges and the rooftops for representing the magnetic current perpendicular to the edges are defined over pairs of patches of different sizes (the patches bounded by the edges have a size that is the half of the size of the other patches).
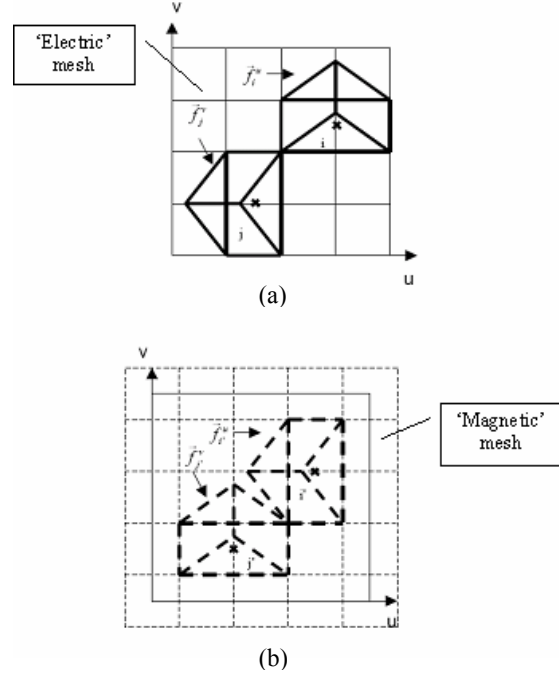


(a)



(b)

Fig. 3. (a) shows an example of rooftops for the u-component, $\vec{f}_{Ei}^u(\vec{r})$, and for the v-component of the electric current, $\vec{f}_{Ej}^v(\vec{r})$. (b) shows an example of the dual rooftops $\vec{f}_{Mj}^u(\vec{r})$ and $\vec{f}_{Mi}^v(\vec{r})$ used to represent the u and v-components, respectively, of the magnetic current. It can be noticed that the rooftops for the electric and magnetic components are defined in dual meshes and that the rooftop for the u-component/v-component of the electric current and the rooftop for the v-component/u-component of the magnetic current have the same centre.

## IV. RESULTS

Figure 7 shows the condition number, [18], versus frequency for a sphere with a radius of 1.m for the single and the dual mesh schemes. Ten subdomains per wavelength were considered in both approaches. The meshes for the electric current were the same in both approaches. The results for the single and the dual mesh schemes were obtained considering PEC and a surface impedance of 1 Ohm, respectively.

A step of 10 MHz was used in the frequency sweep. In the frequency range considered we have two interior resonances at frequencies very close to the two large peaks. It can be appreciated that the dual mesh approach has a better behavior because the condition number for this approach is quite less than for the simple EFIE. As shown in [18] a reduction in the condition number means better convergence and more accurate results. Figure 8 presents the Bi-static RCS results for the co-polar plane cut obtained using the dual approach for the sphere at a frequency of 200 MHz, which is very close to the first internal resonance. A number of 20 divisions per wavelength and a surface impedance of 1 Ohms were considered. The results were obtained with a residual error of $10^{-3}$, which was reached after 965 iterations of the BICGSTAB (L) method, [22], with L=5, which has been used to solve all the MM system of equations in this work. The total number of unknowns was 4836. The numerical results obtained using the dual mesh approach are compared with analytical results derived from the Mie series. A very good accuracy of the numerical results for a frequency very close to an internal resonance was obtained.
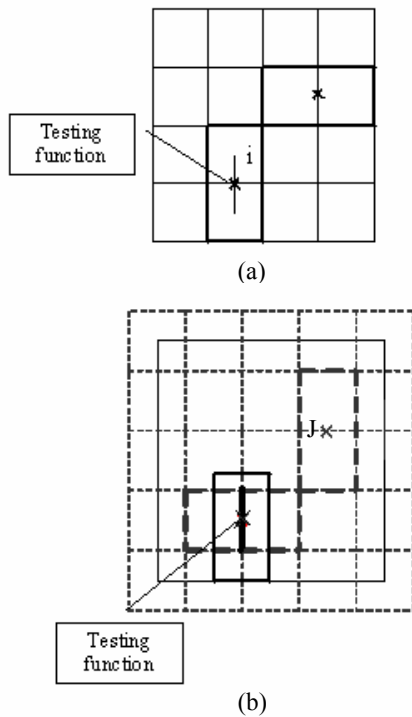


(a)



(b)

Fig. 4. a) The areas covered by the electric rooftops *i* and *j* are indicated by solid lines. The MM impedance term $Z_{ij}^J$ that gives the coupling between rooftop *j* (active) and i (passive) is computed considering a blade-function as a testing function that extends along the segment indicated in the center of rooftop *i*. B) The dual magnetic rooftops are represented by dashed lines. The testing function of the electric rooftop i is a segment that cuts transversally the dual magnetic rooftop.
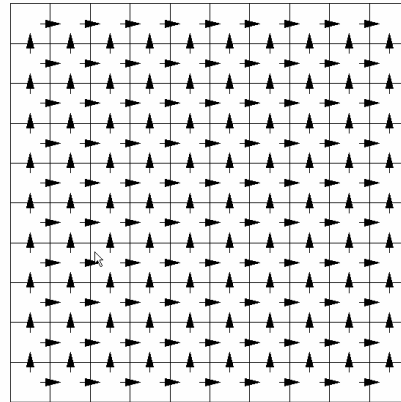


Fig. 5. Mesh used to represent the electric current in a plate. Each arrow corresponds to an electric rooftop.
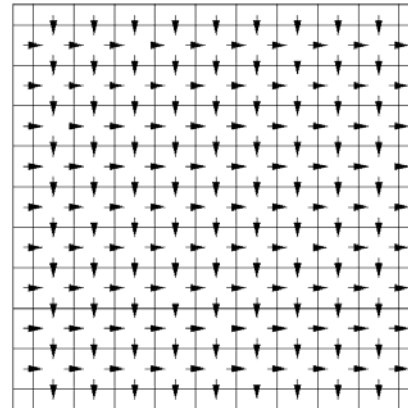


Fig. 6. Mesh used to represent the magnetic current in a plate. Each arrow corresponds to a magnetic rooftop.

In order to show the capacity of the proposed approach to treat coated conducting bodies the case indicated in Fig. 9 was chosen. Numerical and analytical values of the Bi-static RCS are compared in Fig. 9 for the E-plane cut. The surface impedance of the coat is Zs=j72.75 and the current is represented by 20 subdomains per wavelength. The numerical results for the coated sphere are obtained after 780 iterations with an error of $10^{-3}$.

The second structure considered is a very sharp metallic wedge. This geometry gives a very ill-conditioned problem when a plane wave is incident in a direction perpendicular to the edge of the wedge, with the E-field normal to that edge, as indicated in the sketch of Figure 10. The geometry of the problem is defined by two plates of size 1 m × 1 m. In the back part of the wedge the plates are separated by 1.0 cm. The working frequency is 300 MHz. The Bi-static RCS results obtained using the EFIE with a single mesh and with the proposed dual mesh are shown in Figs. 11and 12, respectively. The plates were treated as PEC with the simple mesh approach and with a 1 Ω

surface impedance with the dual mesh approach. A slow convergence of the results is apparent when the number of subdomains per wavelength is changed for the single mesh case in contrast with the fast convergence of the dual mesh case. The results of both formulations converge to nearly the same values for the higher values of divisions per wavelength as shown in Fig. 12. However, the efficiency of the formulations is quite different. As shown in Table 1, the single mesh formulation needs a number of iterations greater than the dual approach for obtaining a residual error of $10^{-3}$.
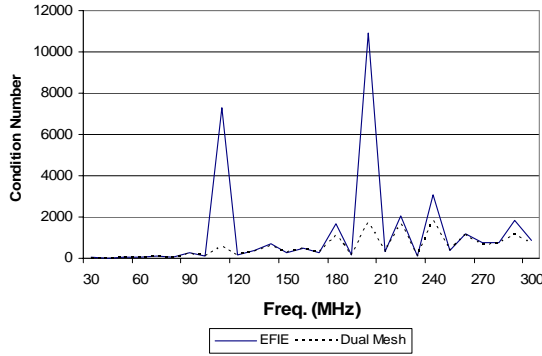


Fig. 7. Condition number versus frequency for a conducting sphere of radius 1 m.
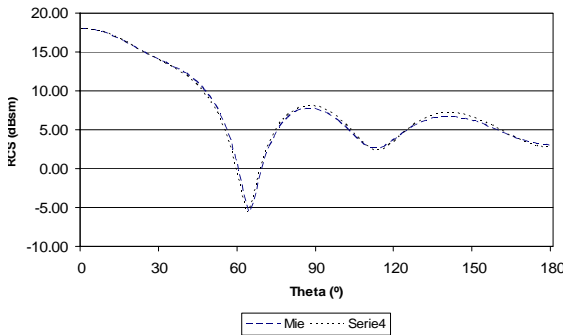


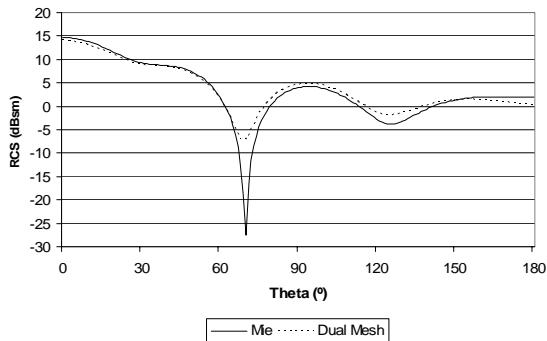Fig. 8. Bi-static RCS results for a conducting sphere of radius 1 m, frequency 200 MHz.



Fig. 9. Bi-static RCS results at a frequency of 300 MHz for a coated PEC sphere with an external radius 0.6 m. The coat is 0.03 m thick and has a relative permittivity of 2.0.
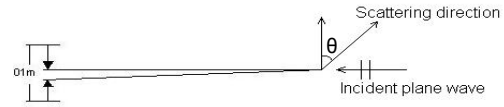


Fig. 10. Wedge geometry considered to compute the Bi-static RCS for a phi-cut = 0º, theta varying from 0º to 180º for an incident plane wave in the direction shown and perpendicularly polarized to the edge of the wedge.
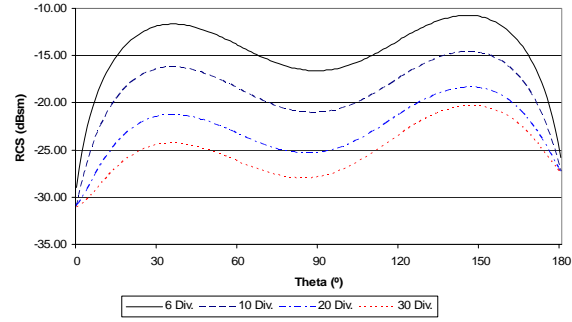


Fig. 11. Bi-static RCS results of the wedge shown in Fig. 10 obtained using the EFIE with a simple mesh for different number of subdomains per wavelength.
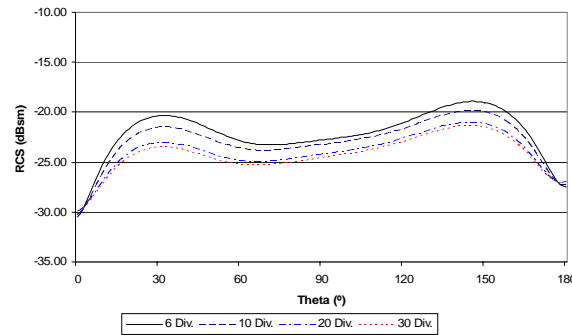


Fig. 12. Bi-static RCS results of the wedge shown in Fig. 10 obtained using the dual mesh approach for different number of subdomains per wavelength.

Table 1. Comparison between the numbers of iterations required for the single and dual mesh approaches for obtaining a residual error of $10^{-3}$ for different sampling densities for the wedge case.

| Subdomains per wavelength | Single Mesh | Dual Mesh |
|---|---|---|
| 6 | 2.061 | 1.310 |
| 10 | 19.189 | 2.495 |
| 20 | 19.304 | 3.388 |
| 30 | 20.684 | 4.460 |

The following case considered is of a rotor structure shown in Fig. 13. This structure is the bottom part of the CHANNEL cavity from ONERA. The height of the structure is 13.7 cm and the external cylinder has a diameter of 18.8 cm. This cylinder has

been modelled as a volumetric structure with a 2 mm of thickness. The blades have a thickness of about 4 mm. The coordinates system has been fixed considering the z axis in the rotor axis. As can be noticed the rotor is a structure with lots of electrically thin plates oriented in many directions, and is quite a difficult problem for the EFIE because it presents lots of thin wedges and therefore it is an interesting problem for testing the efficiency of the dual mesh approach. Figures 14 and 15 show results of the Bi-static RCS of the rotor structure for a frequency of 3.0 GHz and for a θ=0º incidence. Again, the plates were treated as PEC with the simple mesh approach and with 1.Ω of surface impedance with the dual mesh approach. Results were obtained from different values of the sampling density. Table 2 shows the convergence rate for both approaches. It is evident that the dual approach convergence rate always is better than the simple mesh approach.
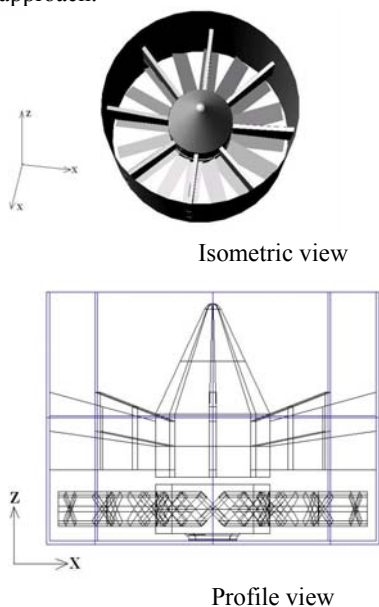


Isometric view



Profile view

Fig. 13. Isometric and profile views of the rotor located at the end of the engine cavity "CHANEL" from ONERA.
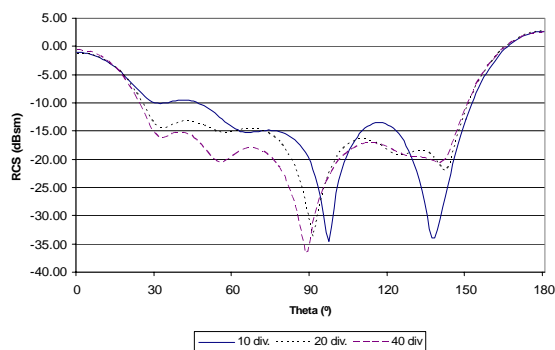


10 div. ······· 20 div. ─ ─ ─ 40 div

Fig. 14. Bi-static RCS results of the CHANEL rotor obtained using the EFIE approach for different subdomain densities.



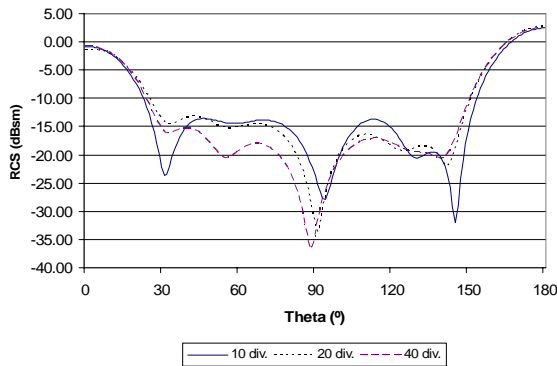10 div. ······· 20 div. ─ ─ ─ 40 div.

Fig. 15. Bi-static RCS results of the CHANEL rotor obtained using the dual mesh approach for different subdomain densities.

Table 2. Comparison between the numbers of iterations required for the single and dual mesh approach for obtaining a residual error of $10^{-3}$ for different sampling densities for the CHANEL rotor case.

| Subdomains per wavelength | Single Mesh | Dual Mesh |
|---|---|---|
| 10 | 465 | 399 |
| 20 | 4.233 | 3.950 |
| 30 | 9.325 | 8.127 |

## V. CONCLUSIONS

A new approach to solve the EFIE using a MM formulation based on dual meshes and on the IBC has been presented. Each mesh is defined by a grid of quadrangles. The meshes are dual because the quadrangle corners of one mesh are the centers of the quadrangles of the other mesh and vice versa. One of the meshes is used to represent the electric current and the other the magnetic current. In both meshes rooftop and razor-blade functions are used as basis and testing functions, respectively. This choice of the basis and testing functions enforces the duality of the formulation: the segment on which the testing function of one mesh extends is perpendicular and completely crosses the basis function of the other mesh. This fact is important because it makes the computation of the electric field due to a magnetic current more easy and accurate.

Any body over which the IBC applies can be treated with the dual mesh formulation including realistic conducting bodies and lossy dielectric bodies. PEC bodies can be analyzed with a very small error by assuming they present small surface impedances, for example a thousandth of the free space wave impedance. All these bodies can be analyzed very efficiently using this method because it requires a lower number of subdomains per wavelength and it

presents better convergence when the MM system of equations is solved by an iterative method. Using the IBC approach we only shall consider the electric current unknowns. The approach is useful to solve structures with open or closed surfaces and it does not suffer a loss of convergence at the frequencies of the internal resonances or other classes of problems, for instance ill-conditioning due to very narrow wedges. In the future the potentiality of the dual mesh approach will be extended to solve the CFIE.

## ACKNOWLEDGEMENTS

## REFERENCES

[1] W. C. Chew, J. Jin, E. Michielssen, and J. Song, *Fast and Efficient Algorithms in Computational Electromagnetics*, Artech House Inc. 2001.

[2] J. R. Mautz and R. F. Harrington, "H-field, E-field, and Combined-Field Solutions for Conducting Bodies of Revolution," AEU, vol 32, pp. 157-164, 1978.

[3] W. D. Wood Jr *et al*, "Convergence Properties of the CFIE for several Conducting Scatterers," *Proceedings of Applied Computational Electromagnetics*, Monterey, CA, pp 677-682, March 2000.

[4] R. A. Shore and A. D. Yaghjian, "Dual-Surface electric Integral Equation," Air *Force Research Laboratory* Rep. AFRL-SN-HS-TR-2001-013, 2001.

[5] V. V. S. Prakash and R. Mittra, "Dual Surface Combined Field Integral Equation for Three-Dimensional Scattering," *Microwave and Opt. Tech. letts.,* vol. 29, pp. 293-296, June 2001.

[6] R. A. Shore and A. D. Yaghjian, "Dual-Surface Integral Equation in Electromagnetic Scattering," *IEEE Trans. Antennas and Propag.*, vol. 53, pp. 1706-1709, May 2005.

[7] J. M. Rius, E. Úbeda, and J. Parrón, "On The Testing of the Magnetic Field Integral Equation With RWG Basis Functions in Method of Moments," *IEEE Trans. Antennas and Propag.*, vol. 49, pp. 1550-1553, November 2001.

[8] E. Ubeda and J. M. Rius, "Novel monopolar MFIE MoM-discretization for the scattering analysis of small objects," *IEEE Trans. Antennas and Propag.*, vol. 54, pp. 50-57, January 2005.

[9] S. Lee and W. Gee, "How good is the impedance boundary condition?," *IEEE Trans. Antennas and Propag.,* vol. 35, pp. 1313-1315, November 1987.

[10] T. B. A. Senior and J. L. Volakis, "Approximate boundary conditions in electromagnetics," *The Institution of Electrical Engineers*, 1995.

[11] Y. Rahmat-Samii and D. J. Hoppe, "Impedance Boundary Conditions in Electromagnetics," *Hemisphere Pub.*, 1995.

[12] O. Gutierrez, J. Bueno, I. Gonzalez, and F. Catedra, "An Improvement of the Method of Moments Combining EFIE and MFIE Formulations for Coated Conducting Bodies," *2005AP/S-URSI International Symposium, Washington*, July 2005.

[13] A. W. Glisson and D. R. Wilton, "Simple and Efficient Numerical Methods for Problems of Electromagnetic Radiation and Scattering from Surfaces," *IEEE Trans. Antennas and Propag.*, vol. 28, pp. 593-603, October 1997.

[14] G. Farin, *Curves and Surfaces for Computer Aided Geometric Design: A practical Guide*, Academic Press.

[15] L. Valle, F. Rivas, and M. F. Cátedra, "Combining the Moment Method with Geometrical Modelling by NURBS Surfaces and Bezier Patches," *IEEE Trans. Antennas and Propag.*, pp. 373-381, March 1994.

[16] F. Rivas, L. Valle, and M. F. Cátedra, "A moment method formulation for the analysis of wire antennas attached to arbitrary conducting bodies defined by parametric surfaces," *Journal of Applied Computational Electromagnetics Society Journal.* pp. 32-39, July 1996.

[17] M. F. Cátedra, F. Rivas, and L. Valle, "A Moment Method Approach Using Frequency Independent Parametric Meshes," *IEEE Trans. Antennas and Propag.*, pp. 1567-1568, October 1997.

[18] C. A. Klein and R. Mittra, "An Application of the 'Condition Number' Concept to the Solution of Scattering Problems in the Presence of the Interior Resonances Frequencies," *IEEE Trans. Antennas and Propag.*, vol. 23, pp. 431-435, May 1975.

[19] G. A. Deschamps and H. S. Cebayan, "Antenna Synthesis and Solution of Inverse Problems by Regularization Methods," *IEEE Trans. Antennas and Propag.*, vol. 20, pp. 268-274, May 1972.

[20] M. H. Smith and A. F. Peterson, "Numerical Solution of the CFIE Using Vector Bases and Dual Interlocking Meshes," *IEEE Trans. Antennas and Propag.*, vol. 53, pp. 3334-3339, October 2005.

[21] C. Balanis, *Advanced Engineering Electromagnetics,* John Wiley&Sons, 1989, New York.

[22] G. L. G. Sleijpen and D. R. Fokkema, "BICGSTAB(L) For Linear Equations

Involving Unsymmetric Matrices With Complex Spectrum," *Electronic Transactions On Numerical Analysis,* vol. 1, pp. 11-32, September 1993.

**Manuel F. Catedra** received his M.S. and Ph. D. degrees in Telecommunications Engineering from the Polytechnic University of Madrid (UPM) in 1977 and 1982 respectively. From 1976 to 1989 he was with the Radiocommunication and Signal Processing Department of the UPM. He has been Professor at the University of Cantabria from 1989 to 1998. He is currently Professor at the University of Alcalá, in Madrid, Spain.

He has worked on about 60 research projects solving problems of Electromagnetic Compatibility in Radio and Telecommunication Equipment, Antennas, Microwave Components and Radar Cross Section and Mobile Communications. He has developed and applied CAD tools for radio-equipment systems such as Navy-ships, aircraft, helicopters, satellites, the main contractors being Spanish or European Institutions such as EADS, ALCATEL, CNES, ALENIA, ESA, DASA, SAAB, INTA, BAZAN, INDRA, the Spanish Defence Department.

He has directed about 15 Ph. D. dissertations, has published about 45 papers (IEEE, Electronic Letters, etc), two books, about 10 chapters in different books, has given short courses and has given around a hundred and thirty presentations in International Symposia.

**Oscar Gutiérrez Blanco** was born in Torrelavega, Spain, in 1970. He received the BS and MS degrees in Telecommunications Engineering from the University of Cantabria, Spain, in 1993 and 1996, respectively. From 1995 to 1998, he was with the Communications Engineering Department of the Cantabria as Research assistant. He received the Ph. D. degree in Telecommunication from the Alcala university, Spain, in 2002. From 1998 to 2000, he was with the Signal Theory and communications Deparment of the Alcala University, Madrid. In 2001, he is currently an assistant professor in the Computational Science Department in the Alcalá University, Madrid.

He has participated in more than 40 research projects, with Spanish and European companies, related with analysis of on board antennas, radio propagation in mobile communication, RCS computation, etc. His research interests are in high-frequency methods in electromagnetic radiation and scattering, and ray-tracing acceleration techniques.

**Iván González Diego** was born in Torrelavega, Spain in 1971. He received the B.S. and M.S. degrees in telecommunications engineering from the University of Cantabria, Spain, in 1994 and 1997 respectively, and the Ph. D. degree in telecommunications engineering from the Univeristy of Alcalá , Madrid, Spain in 2004. He worked in the Detectability Laboratory of the National Institute of Technical Aerospace (INTA), Madrid, Spain and as an Assistant Researcher at the University of Alcalá. He currently works as Assistant Professor in this university. He has participated in several research projects with Spanish and European companies, related with analysis of on board antennas, radio propagation in mobile communications, RCS computation, etc. His research interests are in numerical methods applied to the electromagnetic problems, like genetic algorithms and numerical methods to represent complex bodies for the electromagnetic techniques.

**Francisco Saez de Adana** was born in Santander, Spain, in 1972. He received the BS, MS and Ph. D. degrees in Telecommunications Engineering from the University of Cantabria, Spain, in 1994, 1996 and 2000, respectively. Since 1998 he works at the University of Alcalá, first as assistant professor and since 2002 as professor. He has worked as faculty research at Arizona State University from March 2003 to August 2003.

He has participated in more than forty research projects with Spanish, European, American and Japanese companies and universities, related with analysis of on board antennas, radio propagation in mobile communication, RCS computation, etc. He has directed two Ph. D. Dissertations, has published sixteen papers in referred journals and more than 40 conference contributions at international symposia. His research interests are in areas of high-frequency methods in electromagnetic radiation and scattering, on-board antennas analysis, radio propagation on mobile communications and ray-tracing acceleration techniques.